JACC: CARDIOVASCULAR IMAGING VOL. 14, NO. 6, 2021

PUBLISHED BY ELSEVIER

ORIGINAL RESEARCH

Valve Strain Quantitation in Normal Mitral Valves and Mitral Prolapse With Variable Degrees of Regurgitation

K. Carlos El-Tallawi, MD,[a] Peng Zhang, MS,[b] Robert Azencott, PhD,[b] Jiwen He, PhD,[b] Elizabeth L. Herrera, MD,[c] Jiaqiong Xu, PhD,[d] Mohammed Chamsi-Pasha, MD,[a] Jessen Jacob, MD,[e] Gerald M. Lawrie, MD,[f] William A. Zoghbi, MD[a]

ABSTRACT

OBJECTIVES The aim of this study was to quantitate patient-specific mitral valve (MV) strain in normal valves and in patients with mitral valve prolapse with and without significant mitral regurgitation (MR) and assess the determinants of MV strain.

BACKGROUND Few data exist on MV deformation during systole in humans. Three-dimensional echocardiography allows for dynamic MV imaging, enabling digital modeling of MV function in health and disease.

METHODS Three-dimensional transesophageal echocardiography was performed in 82 patients, 32 with normal MV and 50 with mitral valve prolapse (MVP): 12 with mild mitral regurgitation or less (MVP − MR) and 38 with moderate MR or greater (MVP + MR). Three-dimensional MV models were generated, and the peak systolic strain of MV leaflets was computed on proprietary software.

RESULTS Left ventricular ejection fraction was normal in all groups. MV annular dimensions were largest in MVP + MR (annular area: 13.8 ± 0.7 cm^2) and comparable in MVP − MR (10.6 ± 1 cm^2) and normal valves (10.5 ± 0.3 cm^2; analysis of variance: $p < 0.001$). Similarly, MV leaflet areas were largest in MVP + MR, particularly the posterior leaflet (8.7 ± 0.5 cm^2); intermediate in MVP − MR (6.5 ± 0.7 cm^2); and smallest in normal valves (5.5 ± 0.2 cm^2; $p < 0.0001$). Strain was overall highest in MVP + MR and lowest in normal valves. Patients with MVP − MR had intermediate strain values that were higher than normal valves in the posterior leaflet ($p = 0.001$). On multivariable analysis, after adjustment for clinical and MV geometric parameters, leaflet thickness was the only parameter that was retained as being significantly correlated with mean MV strain ($r = 0.34$; $p = 0.008$).

CONCLUSIONS MVs that exhibit prolapse have higher strain compared to normal valves, particularly in the posterior leaflet. Although higher strain is observed with worsening MR and larger valves and annuli, mitral valve leaflet thickness—and, thus, underlying MV pathology—is the most significant independent determinant of valve deformation. Future studies are needed to assess the impact of MV strain determination on clinical outcome.
(J Am Coll Cardiol Img 2021;14:1099-109) © 2021 by the American College of Cardiology Foundation.

From the [a]Cardiovascular Imaging Institute, Houston Methodist DeBakey Heart and Vascular Center, Houston, Texas, USA; [b]Department of Mathematics, University of Houston, Houston, Texas, USA; [c]Department of Anesthesiology, Division of Cardiovascular and Thoracic Anesthesiology, Houston Methodist DeBakey Heart and Vascular Center, Houston, Texas, USA; [d]Methodist DeBakey Heart and Vascular Center, Center for Outcomes Research, Houston Methodist Research Institute, Houston, Texas, USA; [e]Maimonides Heart and Vascular Institute, Department of Cardiology, Brooklyn, New York, USA; and the [f]Department of Cardiovascular and Thoracic Surgery, Houston Methodist DeBakey Heart and Vascular Center, Houston, Texas, USA.
Victoria Delgado, MD, served as Guest Editor for this paper.
The authors attest they are in compliance with human studies committees and animal welfare regulations of the authors' institutions and Food and Drug Administration guidelines, including patient consent where appropriate. For more information, visit the Author Center.

Manuscript received July 14, 2020; revised manuscript received December 15, 2020, accepted January 6, 2021.

ISSN 1936-878X/$36.00 https://doi.org/10.1016/j.jcmg.2021.01.006

ABBREVIATIONS AND ACRONYMS

3D = 3 dimensional

AL = anterior leaflet

K-S = Kolmogorov-Smirnov

LV = left ventricle

LVEF = left ventricular ejection fraction

MR = mitral regurgitation

MV = mitral valve

MVP = mitral valve prolapse

MVP + MR = mitral valve prolapse with significant mitral regurgitation

MVP − MR = mitral valve prolapse without significant mitral regurgitation

PL = posterior leaflet

TEE = transesophageal echocardiography

The mitral apparatus is a complex structure that deforms during left ventricular (LV) systole in a coordinated manner, where anterior leaflet (AL) and posterior leaflet (PL) coaptation are optimized, and tissue stress minimized. Leaflet size, tissue characteristics, and morphology contribute to tissue deformation and to clinical outcome. The saddle-shaped and dynamic mitral annulus also plays an important role in reducing valve stress (1–3). To date, the majority of published reports on mitral valve (MV) strain are based on animal and in vitro studies (4–9). Advancements in 3-dimensional (3D) echocardiography have led to higher spatial and temporal dynamic volumetric imaging of the MV. In an initial attempt at quantitation of patient-specific MV strain, we developed a proprietary software that required manual tagging of the MV throughout systole and tested it in a small pilot study of normal valves and patients with mitral valve prolapse (MVP) and significant mitral regurgitation (MR) (10,11). The advent of new and fast commercially available tissue tracking software that avoids laborious manual tagging, combined with our strain software, allows for the opportunity to expand and explore in vivo MV strain in larger and more diverse patient populations. The objective of the current study was to assess patient-specific MV strain in normal valves and in patients with MVP with different grades of MR and to assess the determinants of MV strain.

METHODS

PATIENT POPULATION. The patient population was prospectively enrolled between May 2017 and May 2018 and included individuals presenting to the echocardiography laboratory at Houston Methodist Hospital scheduled to undergo transesophageal echocardiography (TEE) for indications of primary MR due to MV prolapse and other select clinical indications where the MV and cardiac structure and function would likely be normal based on a recent transthoracic study (e.g., stroke evaluation in sinus rhythm). We defined the MV as normal whenever there was no evidence of leaflet thickening or calcification, mitral annulus calcifications, or MR in the setting of a normal LV size and ejection fraction

FIGURE 1 Stepwise Approach to MV Anatomic and Strain Measurements Using the 3D TEE Acquisition

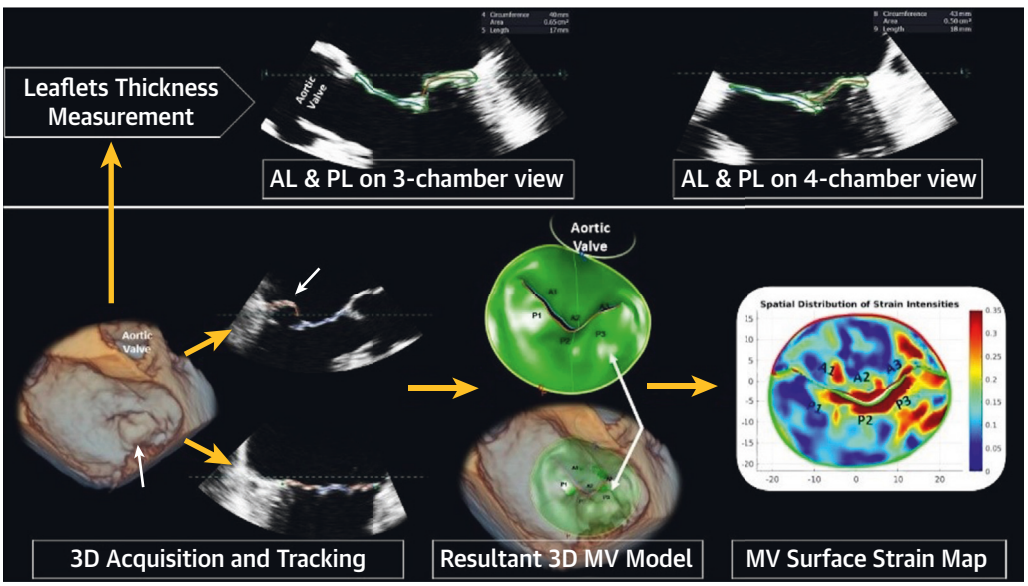

An outline of leaflet thickness measurement **(top)**, along with MV 3D tracking, modeling, and valve strain calculation **(bottom)** using a combination of TomTec's Image Arena software (TomTec Imaging Systems, Unterschleissheim, Germany) (tracking and modeling) and our proprietary software (strain map). The white arrows point to a P2-P3 prolapse **(bottom left)**, which was accurately reproduced on the MV model **(bottom center)**. The MV strain heat map **(bottom right)** reflects the elevated strain posteriorly. 3D = 3 dimensional; AL = anterior leaflet; MV = mitral valve; PL = posterior leaflet; TEE = transesophageal echocardiography.

TABLE 1 Baseline Characteristics and Differences Among Normal MVs and MVP With or Without Significant MR

	Normal Valves (n = 32)	MVP – MR (n = 12)	MVP + MR (n = 38)	p Value
Age, yrs	55.3 ± 2.58	75.9 ± 2.5*	69.18 ± 1.7†	<0.001
Male patients	17 (53)	8 (67)	23 (60)	NS
Body surface area, m^2	2.05 ± 0.05	2.00 ± 0.09	1.97 ± 0.04	NS
Chronic kidney disease	5 (16)	2 (17)	6 (16)	NS
Systolic blood pressure, mm Hg	132.5 ± 4.07	143.8 ± 5.5‡	123.92 ± 5.04	0.08
Diastolic blood pressure, mm Hg	73.43 ± 2.01†	76.4 ± 4.9‡	62.84 ± 2.13	0.001
Heart rate, beats/min	68.9 ± 2.4	69.8 ± 3.7	66.3 ± 2.0	NS
LV ejection fraction, %	63.6 ± 0.6†	61.7 ± 2.1	58.2 ± 1.6	0.03
Regurgitant volume, ml	NA	6.9 ± 1.2	57.1 ± 3.1‡	<0.001
Regurgitant fraction, %	NA	7.3 ± 1.7	47 ± 2‡	<0.001
Effective regurgitant orifice area, cm^2	NA	0.05 ± 0.02	0.42 ± 0.04‡	<0.001

Values are mean ± SE or n (%). *MVP – MR vs. normal valves. †MVP + MR vs. normal valves. ‡MVP – MR vs. MVP + MR ($p < 0.05$ for all).

LV = left ventricular; MV = mitral valve; MVP + MR = mitral valve prolapse with significant mitral regurgitation; MVP – MR = mitral valve prolapse without significant mitral regurgitation; MR = mitral regurgitation; NA = not applicable; NS = not significant.

(LVEF) and normal left atrial size in sinus rhythm. MVP was defined as present when either or both mitral leaflets were seen billowing by ≥2 mm into the left atrium, as per the currently accepted definition (12,13). Exclusion criteria included patients with prosthetic valves, MV endocarditis, or suboptimal images (8 studies in total were excluded; n = 2 in normal valves, and n = 6 in MVP). Blood pressure and heart rate were recorded at the time of 3D TEE acquisition. LVEF was determined either from the TEE or from the most recent transthoracic echocardiogram or cardiac magnetic resonance study (the majority within 7 days of the TEE study). Baseline demographic and clinical data were obtained at the time of enrollment. The study was approved by the human research review board of Houston Methodist Hospital. All patients provided written informed consent for the study before undergoing the TEE.

THE 3D ECHOCARDIOGRAPHY PROTOCOL. The majority of the 3D TEE studies were performed on either the EPIQ or iE33 ultrasound systems (Philips, Andover, Massachusetts) with the X7-2t probe. The imaging protocol consisted of a midesophageal zoom 3D volume acquisition that included the full extent of the mitral annulus, ALs and PLs, and the aortic annulus throughout the cardiac cycle. The acquisition protocol was adjusted for each study to maximize the frame rate while maintaining an adequate spatial resolution; this was performed preferentially using multibeat stitched acquisitions or the high-volume rate feature of iE33 and EPIQ machines when the multibeat attempt caused a significant stitching artifact. (The mean 3D framerate was 33.6 frames/s.) The 3D images were digitally stored as part of each study for postprocessing and off-line analysis. MR severity was quantitated by using regurgitant volume, regurgitant fraction, and effective regurgitant orifice area from the index TEE or a recent (within 7 days) transthoracic echocardiogram, in accordance with the American Society of Echocardiography (14).

PATIENT-SPECIFIC MV TRACKING AND MODELING. Patient-specific models of the motion of the MV annulus and leaflets throughout systole were generated off-line from the 3D TEE datasets using TomTec Image-Arena, version 4.6, software (TomTec Imaging Systems, Unterschleissheim, Germany). The TomTec software automatically segments out the leaflets and annulus on each 3D image frame throughout systole, with minor operator adjustments afterwards. The resultant MV discretized graphic representations generate a mathematical mesh of 800 to 1,000 points of the MV on each image frame (**Figure 1**). Additionally, each MV model contains the respective total and specific leaflet area and annulus circumference and area, along with annular anteroposterior diameter and height.

MV LEAFLET THICKNESS. The thickness of the ALs and PLs was manually calculated by using TomTec Image-Arena, version 4.6, software, as shown in **Figure 1**. In summary, the contour of each leaflet—as delineated by the atrial and ventricular surfaces, the leaflet tip, and annular insertion point—was traced, and its 2-dimensional cross-sectional area was determined. Additionally, the leaflet tip to annular insertion distance (leaflet length) was measured. Leaflet thickness was then calculated as the ratio of leaflet cross-sectional area to leaflet length. These measurements were performed on both the 4-chamber (midesophageal 0°) and 3-chamber

TABLE 2 Mitral Valve Geometric Variables and Differences Among the Groups

	Normal Valves	MVP – MR	MVP + MR	p Value
MV annulus				
Area in projection, cm^2	10.51 ± 0.34	10.6 ± 1.0	13.85 ± 0.75*‡	<0.001
Circumference, cm	11.97 ± 0.19	11.9 ± 0.58	13.62 ± 0.36*†	<0.001
Height, cm	0.74 ± 0.03	0.7 ± 0.06	0.78 ± 0.04	NS
A-P diameter, cm	3.47 ± 0.07	3.45 ± 0.16	3.91 ± 0.10*†	<0.005
MV leaflets				
AL thickness, mm	1.6 ± 0.05	2.2 ± 0.12‡	2.6 ± 0.11*	<0.0001
PL thickness, mm	2.0 ± 0.08	2.4 ± 0.17‡	3.1 ± 0.12*†	<0.0001
AL area, cm^2	6.8 ± 0.23	5.86 ± 0.63	7.64 ± 0.45†	0.047
PL area, cm^2	5.55 ± 0.23	6.50 ± 0.67	8.66 ± 0.52*†	<0.0001
PL/AL area ratio	0.84 ± 0.04	1.15 ± 0.09‡	1.20 ± 0.06*	<0.0001

Values are mean ± SE. *MVP + MR vs. normal valves. †MVP + MR vs. MVP – MR. ‡MVP – MR vs. normal valves ($p < 0.05$ for all).

A-P = anterior-posterior; AL = anterior leaflet; PL = posterior leaflet; other abbreviations as in Table 1.

(midesophageal 120°) views, and the maximum thickness measurement for each leaflet was chosen. The mean MV thickness was defined as the average thickness of the AL and PL.

MV STRAIN COMPUTATION. Because the commercial software does not provide detailed pointwise tracking of mitral leaflet motion, we have developed a proprietary software to compute pointwise tracking of leaflet dynamic deformation between mid- and end systole (15–17). Our software can then compute the midsystolic to end-systolic tissue isotropic strain IS(x) at roughly 800 to 1,000 MV leaflet points x, with no assumptions on tissue elasticity. Computation of strain is detailed in the Supplemental Appendix. In brief, for each leaflet point x and any small leaflet patch P(x) around x, the computed deformation of P(x) between midsystole and end systole roughly multiplies lengths by a dimensionless factor s(x), called the geometric strain at x (17). The isotropic strain IS(x) at x is defined as the magnitude of length dilation (or contraction) around x, given by $IS(x) = |s(x) - 1|$. The isotropic strain computed at nearly 800 points per leaflet characterize the distribution of IS values on the leaflet surface. These patient-specific strain maps are then graphically displayed on the midsystolic 3D image of the MV (Figure 1). Strain was quantitated for the AL, the PL, and the total MV leaflet. In the few patients with atrial fibrillation, because there is a potential for beat-to-beat variability in strain, the beat that best represented the average heart rate was chosen to calculate strain.

HIGH STRAIN CONCENTRATION IN REGIONS OF THE MV. To study the patient-specific highest strain and its localization in both leaflets and regions of the leaflets, we defined 6 geometric regions of interest, corresponding to the 3 scallops of each of the AL and PL (medial, central, and lateral thirds of the corresponding leaflet area). This methodology was previously used and was explained in further detail in our prior publication (10). High strain was defined as larger than that of the patient-specific 75th percentile. A mean high strain concentration was computed for each scallop.

REPRODUCIBILITY. Interobserver and intraobserver reproducibilities of MV modeling and strain calculations were performed in a total of 10 cases. Inter- and intraobserver strain values for the AL and PL, as well as total MV strain, were compared and correlated.

STATISTICAL ANALYSIS. For each patient and each MV leaflet, we have systematically computed 50 quantiles of the patient's leaflet strain values. This has enabled the automatic comparison of strain distributions among patients, both within and across patient groups. To quantify similarity or dissimilarity between any 2 strain distributions, we have implemented the Kolmogorov-Smirnov (K-S) test with correlated data. For each MV leaflet, the correlations between the 800 leaflet strain values are nonzero but remain fairly small. However, when one compares 2 such samples of strain values by a K-S test, small correlations within each sample may weakly impact the p value. We have mitigated this impact by classic corrections to KS-test p values (18). Mean regional high strain concentrations of scallop-affected lesions were compared to normal valves by using the Wilcoxon signed rank test. Values of demographic data and geometric parameters are expressed as mean ± SE. The Fisher exact test (categorical variables) and 1-way analysis of variance (continuous variables) were used to compare patients among the MR severity groups. Pairwise comparisons were adjusted by using a Bonferroni correction to account for multiple comparisons. Univariable linear regression models were used to examine the association between each demographic and clinical variable with MV strain. All statistically significant variables in the univariable model ($p < 0.10$) were then entered to the multivariable linear regression model. The final model was obtained from a backward selection procedure with the significance level for removal from the model of 0.05. Interoperator and intraoperator reproducibility were assessed by intraclass correlation coefficient from 2-way mixed-effects models. All analyses were performed with Stata, version 16 (StataCorp, College Station, Texas). Statistical significance was defined as 2-tailed $p < 0.05$ for all tests.

RESULTS

PATIENT POPULATION. The study population included a total of 82 individuals: 32 with normal MVs and 50 patients with MVP: 12 with mild MR or less (MVP − MR) and 38 with moderate MR or greater (MVP + MR). Of the 12 patients with MVP − MR, 7 had mild MR, 7 (58%) had PL prolapse, 2 (17%) had AL prolapse, and 3 (25%) had bileaflet prolapse. Of the 38 patients with MVP + MR, 26 had severe MR. Underlying lesions were a flail leaflet in 31 and prolapse in 7 patients. In both MVP groups, a total of 67 valve lesions were identified with the majority of those located in the PL (n = 40; 60%), 8 were in the AL (12%), 5 had bileaflet prolapse (7%), and 4 had commissural lesions (6%). Finally, 6 patients were in atrial fibrillation during the image acquisition.

Table 1 details the characteristics of the study groups. The mean age was lower in the normal group. LVEF was normal in all the groups but lowest in MVP + MR. Systolic blood pressures and heart rates were comparable among all the groups.

GEOMETRY OF THE MV ANNULUS AND LEAFLETS. The geometric parameters of the mitral valve apparatus are detailed in Table 2. MV annular area was largest in MVP + MR and comparable between MVP − MR and normal valves. The same relationship was noted for annular circumference and anterior-posterior diameter. The MVP + MR group had the largest leaflet areas compared to MVP − MR and normal valves. Of interest, the PL area in both MVP groups was larger than the AL area so that the PL/AL area ratio was >1 and was significantly larger than in normal valves. The thickness of the MV was higher in MVP compared to normal valves and exhibited a progressive increase in both leaflets from normal valves, to MVP − MR, to MVP + MR.

MV LEAFLET STRAIN. Mean strain values for each leaflet and the whole MV in each patient group are depicted in Figure 2. Mean strain values were significantly higher in the PL compared to the AL in all 3 groups: normal valves (9.3 ± 0.4% vs. 7.6 ± 0.3%), MVP − MR (11.5 ± 0.6% vs. 8.5 ± 0.5%), and MVP + MR (13.3 ± 0.4% vs. 10.8 ± 0.4%). Valve strain was highest in MVP + MR, intermediate in MVP − MR, and lowest in normal valves for each leaflet and the total MV (total MV strain: 12 ± 0.3%, 10 ± 0.4%, and 8.5 ± 0.2%, respectively; p < 0.005).

Figure 3 depicts the detailed regional distribution of strain on the surface of each leaflet for the 3 groups, represented as percentile strain curves. Strain map patient examples from each group are also shown. The MVP + MR group had the highest valve strain, whereas normal valves had the lowest strain on both leaflets. MVP − MR strain values were comparable to normal valves on the AL (K-S: p = 0.38) but higher (K-S: p = 0.001) and comparable to MVP + MR (K-S: p = 0.19) on the PL.

FIGURE 2 Leaflet and Total MV Mean Strain Values in Normal Valves and in MVP − MR and MVP + MR

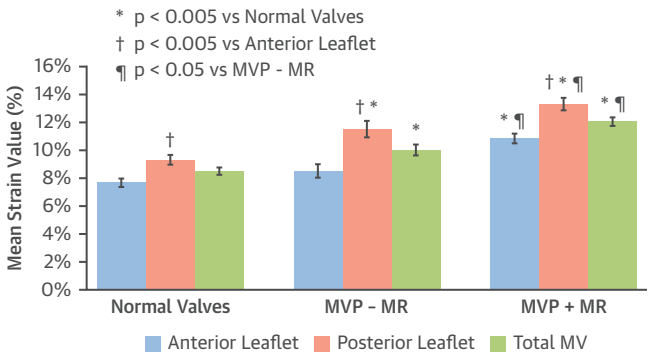

Mean strain of the posterior leaflet is consistently higher than the anterior leaflet across all groups. Mean total MV strain is highest in MVP + MR, intermediate in MVP − MR, and lowest in normal valves. MV = mitral valve; MVP + MR = mitral valve prolapse with significant mitral regurgitation; MVP − MR = mitral valve prolapse without significant mitral regurgitation.

REGIONAL STRAIN IN PROLAPSING SCALLOPS. In the groups with MVP (n = 50), prolapse occurred mostly in the PL in 40 patients (80%), which permitted the analysis of regional strain differences in the involved versus noninvolved scallops. More significant high strain concentrations were observed in the prolapsing P3 scallop compared to the non-prolapsing scallops (p < 0.004) (Figure 4). The same trend was seen for P2 scallop involvement (p = 0.09). Only 4 patients had P1 prolapse; in these patients, high strain concentration was also higher but without attaining statistical significance.

DETERMINANTS OF STRAIN. We sought to determine the potential clinical, echocardiographic, and MV geometric parameters that were best related with mean leaflet strain. On univariable analysis, mean MV thickness, MVP + MR group, total leaflet area, and annulus area were significantly correlated with MV strain (Table 3). On multivariable analysis, mean MV thickness was the only parameter that was retained as being significantly correlated with mean MV strain (p = 0.008). The relationship between mean MV strain and leaflet thickness is depicted in Figure 5 (r = 0.34; p = 0.008). The individual groups are color-coded to highlight the relation of valve thickness and presence/severity of MR with strain.

FIGURE 3 Strain Percentile Distribution for the Anterior MV Leaflet and Posterior Leaflet in Normal Valves and in the MVP Groups

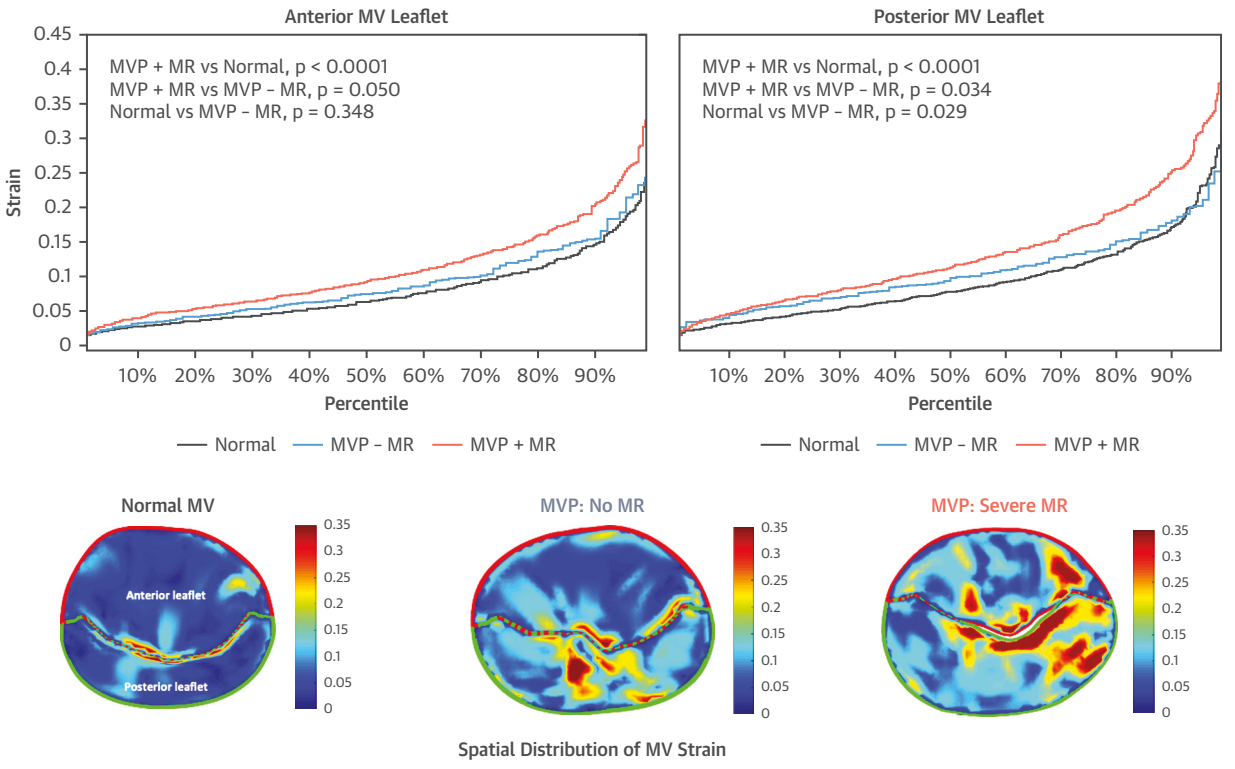

Percentile refers to the percent of the approximately 800 analyzed points on the MVs that have a strain value at or below the respective value on the curve for the group analyzed (e.g., 50th percentile is the median). Highest MV strain values were observed in MVP + MR for both leaflets. Posterior leaflet strain distribution in MVP – MR was lower than MVP + MR; both were significantly higher than normal valves. Examples of MV strain maps from a normal MV, from a patient with MVP with severe MR, and from another patient without MR are also shown. Abbreviations as in Figure 2.

REPRODUCIBILITY. The interoperator strain distribution intraclass correlation (95% confidence interval) was 0.88 (0.82 to 0.92) for the AL and 0.80 (0.71 to 0.86) for the PL. The absolute strain difference was 2.0 ± 0.3% for the AL and 1.7 ± 0.4% for the PL. The intraoperator intraclass correlation was 0.93 (0.89 to 0.95) for the AL and 0.91 (0.89 to 0.95) for the PL, with an absolute strain difference of 1.7 ± 0.2% for the AL and 1.9 ± 0.2% for the PL.

DISCUSSION

This is the first noninvasive study evaluating strain in normal mitral valves and in patients with MVP, spanning the spectrum of MR severity. We determined MV geometric and strain models using a combination of commercially available and proprietary software. Patients with MVP and significant MR had substantial geometric remodeling of the MV apparatus; this was also noted—albeit to a lesser extent and more so at the leaflet level—in the MVP group with no or mild MR. MV strain was consistently higher in the PL in every group. Patients with MVP had higher strain compared to those with normal valves, irrespective of MR presence or severity, particularly on the PL and highest in the prolapsed scallop. Mean leaflet thickness was the major determinant of strain severity, after adjustment for clinical and MV geometric variables (**Central Illustration**).

MV MODELING FOR STRAIN DETERMINATION. Determinations of MV deformation and leaflet tissue elastic properties were based predominantly on animal models where crystals were surgically implanted, and their motion on the valve was tracked with cameras (1,3,4,6). Information on strain distribution on the surface of MV leaflets in humans is limited, involving a small number of patients. The MV annulus with its saddle shape was shown to increase leaflet curvature and contribute to reducing peak leaflet stress in 3 patients (3) and in animal models (3,19,20). Human MV models based on 10 normal

FIGURE 4 Comparison of Regional High Strain Concentration Between Prolapsing and Nonprolapsing Scallops in Posterior Leaflets

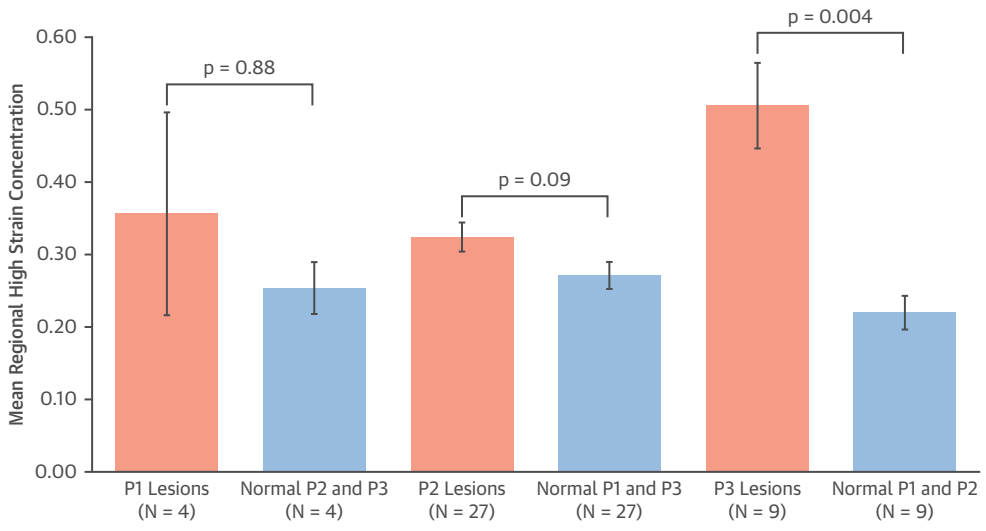

Comparison of regional high strain concentration (patient specific: >75th percentile) in prolapsing and nonprolapsing scallops of the posterior leaflet, showing a tendency for high strain localization to the scallops exhibiting prolapse.

valves were used to emulate mitral leaflet deformation during isovolumic contraction (21). In another study, 3D echocardiographic images of 2 normal valves and 2 patients with MR (7,8) aimed to model valve leaflet strain, assuming that papillary muscles remain at constant distance from the mitral leaflets (22,23). All of the mentioned investigations had to use elasticity model parameters derived from animal data because biomechanical properties of human MV leaflets in vivo are not yet well quantified.

In the present study, we quantitated MV leaflet strain and its regional distribution in healthy and prolapsing mitral valves. We built on the recent pilot observations from our institution (10,11) and present the first data assessing MV strain and its determinants in normal MV and in those with MVP and various degrees of MR severity. The tracking of the MV leaflets was automated, with minimal operator input sometimes required for adjustment of suboptimal tracking—mostly in cases of flail leaflet or significant prolapse with a large malcoaptation/flail gap. The total time spent per valve for the modeling and strain calculations averaged 10 to 15 min. We believe that this time can be further shortened if the modeling and strain tools could potentially be linked together in a single platform.

Patient-specific leaflet deformations were reconstructed by computerized diffeomorphic registration of the 3D echocardiographic images. Computed isotropic strain was then systematically generated by leaflet dynamics at nearly 1,000 points on the MV (24). Quantifying leaflet strain as indicator of MV tissue fatigue has several advantages. First, this approach can be easily implemented for humans through computer analysis of standard 3D echocardiography. Second, we did not need to introduce any elasticity hypotheses of MV leaflet tissue for strain calculation. Indeed, realistic MV elasticity models are anisotropic and highly nonlinear; in most publications, parameterization of elasticity models for human MVs relied on stress measurements made in vivo on animal models. Furthermore, MV elasticity models would be very different in normal valves and in the variable tissue characteristics of MV prolapse. Comparison of MV isotropic strain distributions across patients is robust to reconstruction errors because it relies on percentile curves computed from approximately 800 strain values for each leaflet, so that the error on any strain percentile is 20 times smaller than the errors affecting individual strain values.

STRAIN IN NORMAL VALVES AND IN MV PROLAPSE. In all mitral valves, MV strain was found to be higher in the PL. This could be explained by the lower stiffness on the posterior aspect of the mitral annulus, as demonstrated histologically (25). Using excised porcine valves, May-Newman and Yin (26)

TABLE 3 Univariable and Multivariable Correlates of Mitral Valve Strain From Linear Regression Model

	Estimated Coefficient (95% CI)	p Value
Univariable model		
Age	0.0002 (-0.0004 to 0.0008)	0.512
Systolic blood pressure	-0.0002 (-0.0006 to 0.0001)	0.222
Sex	-0.0050 (-0.0232 to 0.0133)	0.589
Chronic kidney disease	0.0059 (-0.0199 to 0.0316)	0.651
Mean leaflet thickness	0.0195 (0.0054 to 0.0337)	0.008
MR severity		
Normal valves	Ref.	
0–1+ MR	0.0153 (-0.0077 to 0.0382)	0.189
2–3+ MR	0.0276 (0.0076 to 0.0476)	0.008
Total leaflet area	0.0027 (0.0004 to 0.005)	0.022
Annulus area	0.0030 (0.0004 to 0.0056)	0.024
Flail	0.0044 (-0.0179 to 0.0267)	0.695
LVEF	-0.0006 (-0.0021 to 0.0008)	0.379
Multivariable model		
Mean leaflet thickness	0.0195 (0.0054 to 0.0337)	0.008

CI = confidence interval; LVEF = left ventricular ejection fraction; MR = mitral regurgitation.

demonstrated that the PL is more extensible than its anterior counterpart, with significantly higher strain at the same stress. These findings are of clinical interest because the majority of mitral annular calcifications occur in the posterior mitral annulus (27). The repetitive regional deformation of higher magnitude could hypothetically be a contributing mechanism to the observed posterior annular calcifications in the aging MV or in disease states more susceptible to inflammation or calcification, such as renal disease or rheumatoid arthritis.

Deformation of mitral valves with prolapse was found to be significantly higher than that of normal valves and was largest in the MVP + MR group, particularly in the PL. Remodeling of the MV annulus and leaflets was noted in both MVP groups but to different extents, with the MVP – MR group showing changes mostly at the leaflet level (increased leaflet thickness and area), whereas the MVP + MR cohort demonstrated more extensive changes involving both the leaflets and annulus. Despite the statistically similar MV geometric dimensions for normal valves and MVP – MR, strain was higher in the latter group, especially in the PL.

FIGURE 5 Scatterplot of Mean MV Strain Versus Mean Leaflet Thickness, Color-Coded for Each of the Groups

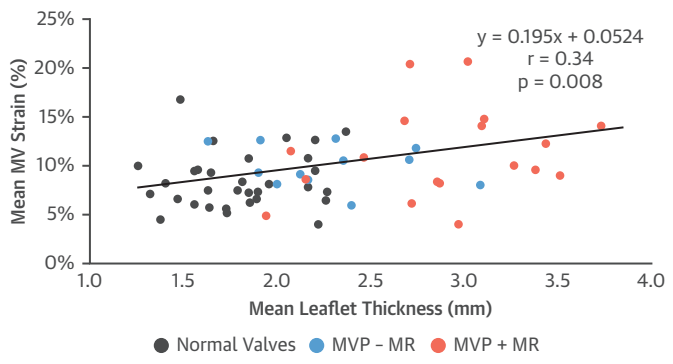

There is a positive correlation between strain and leaflet thickness that remains significant after adjustment for other pertinent variables. MV = mitral valve.

DETERMINANTS OF MV STRAIN. Leaflet thickness and area, MV annulus area, and MR severity correlated significantly with mean MV strain. After adjustment for multiple parameters, mean leaflet thickness was the sole parameter that correlated with strain. Larger MV deformation was seen in thicker, more myxomatous valves. This is plausible with what is known about MVP pathology. In mitral valves with myxomatous degeneration, transforming growth factor-β mediates endothelial-mesenchymal transdifferentiation of endothelial cells into myofibroblasts, promoting increased matrix production along with collagen and elastin degradation within the valvular fibrosa (28–30). The end result is a valve tissue that is thickened, weakened, and more prone to excessive deformation (31), a characteristic captured by leaflet thickness measurements and strain calculations. Therefore, the higher strain observed in MVP + MR, especially versus MVP – MR, could be explained by an inherently more advanced myxomatous degeneration, as reflected by the thicker leaflets, with an added contribution of the larger annulus and leaflet area. In our previous pilot study, the contribution of significant MR to the higher strain could not be excluded because all 10 patients had significant MR (10). In the current series, MVP without significant MR exhibited higher-than-normal strain, intermediate between normal and those with worse myxomatous degeneration, MR, and valve/annular remodeling. Blood pressure, within a physiological range, was not an important determinant of strain, although in extremes, one would predict a direct relationship to strain. It is undeniable that the variables used in the multivariable analysis do not necessarily capture the entirety of the various anatomic, pathological, and hemodynamic contributors to leaflet strain; however, we believe that these were inclusive of the majority of practically attainable strain substrates.

CLINICAL VALIDITY OF THE STRAIN QUANTITATION METHODOLOGY. Diffeomorphic registration has often been applied to 3D cardiac magnetic resonance

CENTRAL ILLUSTRATION **Mitral Valve Strain is Higher in Mitral Valve Prolapse Compared to Normal Valves and Increases With Disease Severity**

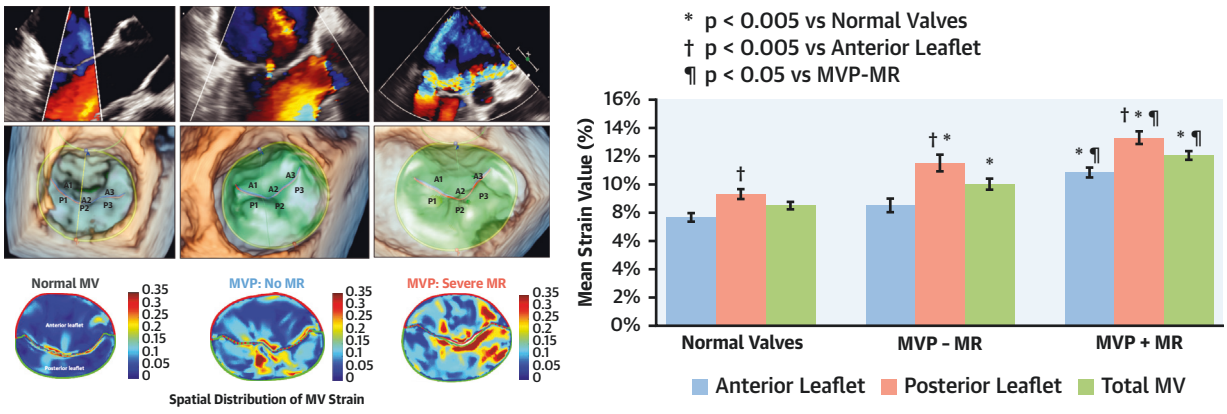

El-Tallawi, K.C. et al. J Am Coll Cardiol Img. 2021;14(6):1099-109.

Mitral valve (MV) strain quantitated with transesophageal echocardiography is higher in the posterior leaflet in normal valves and in mitral valve prolapse (MVP). Strain is higher in MVP compared to normal valves, and increases with disease severity. MR = mitral regurgitation.

sequences of beating hearts to quantitate ventricle geometry, cardiac motion, and myocardial strain (32-35). In our study, image segmentation software (TomTec Image-Arena, version 4.6) locates the surface S(t) of mitral valve leaflets at each frame time t. We then computed a differentiable and invertible deformation from S(t) to S(t + 1), minimizing the kinetic energy of the deformation. Our diffeomorphic registration technique is similar to known and well-established approaches (36,37). We have not directly tested our software on animal models, but the accuracy of cardiac tracking and myocardial strain computed by diffeomorphic registration has been validated versus ground truth on simulated 3D ultrasound images (38) or where synthetic ultrasound image sequences were provided (39). Importantly, the strain parameter is an index that allows comparison of the deformation properties of the MV regionally and globally in heath and disease states affecting the MV.

CLINICAL IMPLICATIONS AND FUTURE DIRECTIONS. Myxomatous degeneration of the MV apparatus is an important factor predisposing to complications (40-42). In this condition, the chordae tendineae are also affected pathologically, predisposing to chordal lengthening, more prolapse, MR, or chordal rupture (31). The mitral prolapse substudy of the Framingham Heart Study demonstrated a strong relation of valve thickness to clinical worsening of initially nondiagnostic MVP morphologies that can evolve to diagnostic MVP over a 3- to 16-year period, confirming the importance of identifying minimal MVP expression (43). These structural histological associations with prognosis (31,40,42,43) are of particular importance in that they theoretically offer the current missing link tying clinical strain data to long-term outcome, be it disease progression or complications. Now that the methodology is available for strain quantitation, longitudinal prospective studies are needed to assess the prognostic impact of MV strain calculation in patients with MVP. In our opinion, MV strain may have a wide array of potential clinical applications, from the diagnosis of early myxomatous degeneration to the prediction of downstream complications (such as chordal rupture in cases with more advanced pathologies with elevated strain), and the potential to predict the success and durability of surgical nonresectional mitral valve repair. To this point, transthoracic echocardiography offers a very attractive tool for large-scale longitudinal studies of the downstream effects and outcomes of MV strain; this can be achieved whenever 3D ultrasound technology attains consistently high spatial resolution for MV imaging from the transthoracic approach.

STUDY LIMITATIONS. First, because TEE is needed at this time for strain calculations, there is an inherent selection bias that we cannot fully control, including a smaller number of MVP – MR, because these patients usually do not require a TEE. Second, mean leaflet thickness has inherent errors because it is

obtained from few representative views (4- and 3-chamber views) and therefore does not represent the mean thickness of the whole MV. We derived the mean thickness from an area-length approach, which does not account for the variable regional valve thickness but decreases the errors of individual thickness measurements at multiple sites. Finally, the multibeat and high-volume rate acquisitions used on 3D TEE may include data from up to 4 consecutive beats. Stitch artifacts were avoided. Although these beats can potentially have variable strain values, we assumed that the differences are negligible because the beats are consecutive.

CONCLUSIONS

This is the first study in humans in which patient-specific MV isotropic strain was quantified in normal valves and in patients with MVP with a full spectrum of MR severity. Patients with MVP had higher strain values compared to normal MV, which was largely determined by leaflet thickness. Valve strain was consistently higher in the PL in normal valves and in those with MVP, which may explain the predilection of the PL and annulus to disease states. Longitudinal studies are needed to assess whether MV strain can predict prognosis in patients with MVP, beyond that of valve structure and thickness.

FUNDING SUPPORT AND AUTHOR DISCLOSURES

Supported by the Elkins Family Distinguished Chair in cardiac health and the John and Maryanne McCormack Cardiology Fund. The authors have reported that they have no relationships relevant to the contents of this paper to disclose.

ADDRESS FOR CORRESPONDENCE: Dr. William A. Zoghbi, Department of Cardiology, Houston Methodist DeBakey Heart and Vascular Center, 6550 Fannin Street, SM 1801, Houston, Texas 77030, USA. E-mail: wzoghbi@houstonmethodist.org. Twitter: @williamzoghbi.

PERSPECTIVES

COMPETENCY IN MEDICAL KNOWLEDGE: The majority of previously published MV leaflet deformation studies were performed in animal models. Our study explores patient-specific quantitation of MV tissue deformation in normal valves and in a cohort of patients with MVP with various degrees of regurgitation using TEE. Patients with MVP had higher valve strain compared to normal valves. Although strain was related to geometric remodeling of the MV apparatus and MR, elevated strain was predominantly a function of valve thickness, reflecting underlying leaflet tissue characteristics.

TRANSLATIONAL OUTLOOK: A quantitative valve strain approach adds to the armamentarium of MV assessment tools by opening a new window to explain the pathophysiology of disease predilection to the posterior valve leaflet and mitral annulus and evaluate whether strain determination can add to clinical outcome beyond that of geometric remodeling of the valve apparatus.

REFERENCES

1. Jimenez JH, Liou SW, Padala M, et al. A saddle-shaped annulus reduces systolic strain on the central region of the mitral valve anterior leaflet. J Thorac Cardiovasc Surg 2007;134:1562–8.

2. Kunzelman KS, Reimink MS, Cochran RP. Annular dilatation increases stress in the mitral valve and delays coaptation: a finite element computer model. Cardiovasc Surg 1997;5:427–34.

3. Salgo IS, Gorman JH 3rd., Gorman RC, et al. Effect of annular shape on leaflet curvature in reducing mitral leaflet stress. Circulation 2002;106:711–7.

4. Rausch MK, Bothe W, Kvitting JP, Goktepe S, Miller DC, Kuhl E. In vivo dynamic strains of the ovine anterior mitral valve leaflet. J Biomech 2011;44:1149–57.

5. Stevanella M, Krishnamurthy G, Votta E, Swanson JC, Redaelli A, Ingels NB Jr. Mitral leaflet modeling: Importance of in vivo shape and material properties. J Biomech 2011;44:2229–35.

6. He Z, Ritchie J, Grashow JS, Sacks MS, Yoganathan AP. In vitro dynamic strain behavior of the mitral valve posterior leaflet. J Biomech Eng 2005;127:504–11.

7. Rim Y, McPherson DD, Chandran KB, Kim H. The effect of patient-specific annular motion on dynamic simulation of mitral valve function. J Biomech 2013;46:1104–12.

8. Rim Y, Laing ST, Kee P, McPherson DD, Kim H. Evaluation of mitral valve dynamics. J Am Coll Cardiol Img 2013;6:263–8.

9. Sacks MS, He Z, Baijens L, et al. Surface strains in the anterior leaflet of the functioning mitral valve. Ann Biomed Eng 2002;30:1281–90.

10. Ben Zekry S, Freeman J, Jajoo A, et al. Patient-specific quantitation of mitral valve strain by computer analysis of three-dimensional echocardiography: a pilot study. Circ Cardiovasc Imaging 2016;9:e003254.

11. Ben Zekry S, Freeman J, Jajoo A, et al. Effect of mitral valve repair on mitral valve leaflets strain: a pilot study. J Am Coll Cardiol Img 2018;11:776–7.

12. Levine RA, Stathogiannis E, Newell JB, Harrigan P, Weyman AE. Reconsideration of echocardiographic standards for mitral valve prolapse: lack of association between leaflet displacement isolated to the apical four chamber view and independent echocardiographic evidence of abnormality. J Am Coll Cardiol 1988;11:1010–9.

13. Addetia K, Mor-Avi V, Weinert L, Salgo IS, Lang RM. A new definition for an old entity: improved definition of mitral valve prolapse using three-dimensional echocardiography and color-coded parametric models. J Am Soc Echocardiogr 2014;27:8–16.

14. Zoghbi WA, Adams D, Bonow RO, et al. Recommendations for noninvasive evaluation of native valvular regurgitation: a report from the American Society of Echocardiography developed

in collaboration with the Society for Cardiovascular Magnetic Resonance. J Am Soc Echocardiogr 2017;30:303–71.

15. Azencott R, Glowinski R, Ramos AM. A controllability approach to shape identification. Appl Math Lett 2008;21:861–5.

16. Azencott R, Glowinski R, He J, et al. Diffeomorphic matching and dynamic deformable surfaces in 3D medical imaging. Comput Methods Appl Math 2010;10:235–74.

17. Zekry SB, Lawrie G, Little S, et al. Comparative evaluation of mitral valve strain by deformation tracking in 3D-echocardiography. Cardiovasc Eng Technol 2012;3:402–12.

18. Weiss MS. Modification of the Kolmogorov-Smirnov statistic for use with correlated data. J Am Stat Assoc 1978;73:872–5.

19. Ryan LP, Jackson BM, Eperjesi TJ, et al. A methodology for assessing human mitral leaflet curvature using real-time 3-dimensional echocardiography. J Thorac Cardiovasc Surg 2008;136:726–34.

20. Ryan LP, Jackson BM, Hamamoto H, et al. The influence of annuloplasty ring geometry on mitral leaflet curvature. Ann Thorac Surg 2008;86:749–60.

21. Xu C, Brinster CJ, Jassar AS, et al. A novel approach to in vivo mitral valve stress analysis. Am J Physiol Heart Circ Physiol 2010;299:H1790–4.

22. Joudinaud TM, Kegel CL, Flecher EM, et al. The papillary muscles as shock absorbers of the mitral valve complex. An experimental study. Eur J Cardiothorac Surg 2007;32:96–101.

23. Sanfilippo AJ, Harrigan P, Popovic AD, Weyman AE, Levine RA. Papillary muscle traction in mitral valve prolapse: quantitation by two-dimensional echocardiography. J Am Coll Cardiol 1992;19:564–71.

24. Slaughter WS, editor. The Linearized Theory of Elasticity. Boston, MA: Springer, 2002.

25. Gunning GM, Murphy BP. Determination of the tensile mechanical properties of the segmented mitral valve annulus. J Biomech 2014;47:334–40.

26. May-Newman K, Yin FC. Biaxial mechanical behavior of excised porcine mitral valve leaflets. Am J Physiol 1995;269:H1319–27.

27. Bloom N, Cashon G. Annulus fibrosus calcification of the mitral valve. Am Heart J 1945;30:619–22.

28. Xu S, Grande-Allen KJ. The role of cell biology and leaflet remodeling in the progression of heart valve disease. Methodist Debakey Cardiovasc J 2010;6:2–7.

29. Cushing MC, Liao J, Anseth KS. Activation of valvular interstitial cells is mediated by transforming growth factor-β1 interactions with matrix molecules. Matrix Biology 2005;24:428–37.

30. Levine RA, Hagége AA, Judge DP, et al. Mitral valve disease—morphology and mechanisms. Nat Rev Cardiol 2015;12:689–710.

31. Barber JE, Kasper FK, Ratliff NB, Cosgrove DM, Griffin BP, Vesely I. Mechanical properties of myxomatous mitral valves. J Thorac Cardiovasc Surg 2001;122:955–62.

32. Cao Y, Miller MI, Winslow RL, Younes L. Large deformation diffeomorphic metric mapping of vector fields. IEEE Trans Med Imaging 2005;24:1216–30.

33. Helm P, Beg MF, Miller MI, Winslow RL. Measuring and mapping cardiac fiber and laminar architecture using diffusion tensor MR imaging. Ann N Y Acad Sci 2005;1047:296–307.

34. Mansi T, Peyrat J, Sermesant M, et al. Physically-constrained diffeomorphic demons for the estimation of 3D myocardium strain from cine-MRI. In: Ayache N, Delingette H, Sermesant M, editors. Functional Imaging and Modeling of the Heart. Heidelberg, Germany: Springer, 2009;5528:201-10.

35. Lombaert H, Peyrat J, Croisille P, et al. Human atlas of the cardiac fiber architecture: study on a healthy population. IEEE Trans Med Imaging 2012;31:1436–47.

36. Wang L, Beg F, Ratnanather T, et al. Large deformation diffeomorphism and momentum based hippocampal shape discrimination in dementia of the Alzheimer type. IEEE Trans Med Imaging 2007;26:462–70.

37. De Craene M, Camara O, Bijnens BH, Frangi AF. Large diffeomorphic FFD registration for motion and strain quantification from 3D-US sequences. In: Ayache N, Delingette H, Sermesant M, editors. Functional Imaging and Modeling of the Heart. Heidelberg, Germany: Springer 2009;5528:437–46.

38. Heyde B, Alessandrini M, Hermans J, Barbosa D, Claus P, D'hooge J. Anatomical image registration using volume conservation to assess cardiac deformation from 3D ultrasound recordings. IEEE Trans Med Imaging 2015;35:501–11.

39. Prakosa A, Mcleod K, Sermesant M, Pennec X. Evaluation of iLogDemons algorithm for cardiac motion tracking in synthetic ultrasound sequence. International workshop on statistical atlases and computational models of the heart. Heidelberg, Germany: Springer; 2012;35:178-87.

40. Avierinos J, Detaint D, Messika-Zeitoun D, Mohty D, Enriquez-Sarano M. Risk, determinants, and outcome implications of progression of mitral regurgitation after diagnosis of mitral valve prolapse in a single community. Am J Cardiol 2008;101:662–7.

41. Nishimura RA, McGoon MD, Shub C, Miller FA Jr., Ilstrup DM, Tajik AJ. Echocardiographically documented mitral-valve prolapse: long-term follow-up of 237 patients. N Engl J Med 1985;313:1305–9.

42. Marks AR, Choong CY, Sanfilippo AJ, Ferré M, Weyman AE. Identification of high-risk and low-risk subgroups of patients with mitral-valve prolapse. N Engl J Med 1989;320:1031–6.

43. Delling FN, Rong J, Larson MG, et al. Evolution of mitral valve prolapse: insights from the Framingham Heart Study. Circulation 2016;133:1688–95.

KEY WORDS echocardiography, mitral valve, mitral valve prolapse, strain, valve regurgitation

APPENDIX For an explanation of the derivation of isotropic mitral valve strain, please see the online version of this paper.